

Structure of Modified Neuropeptides in Relation to the Cell Entering Mechanism

A Major Qualifying Project (MQP) Report
Submitted to the Faculty of
WORCESTER POLYTECHNIC INSTITUTE
in partial fulfillment of the requirements
for the Degree of Bachelor of Science in

Physics,
Biology and Biotechnology

By:

Allison Hershoff
Benjamin Lunden

Project Advisors:

Izabela Stroe
Jagan Srinivasan

Date: April 2021

This report represents work of WPI undergraduate students submitted to the faculty as evidence of a degree requirement. WPI routinely publishes these reports on its website without editorial or peer review. For more information about the projects program at WPI, see <http://www.wpi.edu/Academics/Projects>.

Abstract

Neuropeptides are essential to neuron function and significantly affect behavioral response. While neuropeptides are beneficial for behavior, at high concentrations they can be detrimental to cell function. Recent research shows that amino acid substitutions in neuropeptides could lead to changes in the cell entering mechanisms. We investigated the structure-function of modified neuropeptides families of FaRP (FLP-3-2 and FLP-3-9) and TRH (TRH-1A and TRH-1B) using dielectric relaxation spectroscopy (DRS) and circular dichroism (CD). We measured the complex dielectric permittivity and conductivity of the neuropeptides in the frequency range 200mHz to 40MHz at 0.5 μ M and 1 μ M. We determined the structure of the neuropeptides using CD data and compared it to computational models. We found that the longer amino acids chain neuropeptide FLP-3-9 has a lower permittivity than FLP-3-2. A decrease in permittivity was also observed when the Arginine and Glycine were substituted with Asparagine and Alanine in TRH. Knowing the complete structure and function of modified neuropeptides leads to further complex sequencing of TRH and FLP in neurobiology.

Acknowledgements

We would like to thank Elizabeth DiLoreto in Professor Srinivasan's laboratory for supplying the neuropeptides from Biomatik and Professor Dmitry Korin for generating the neuropeptide structures. We would also like to thank Elizabeth van Zyl and Daryl Johnson for CD instructions and safety.

Contents

1	Introduction	1
1.1	Peptide Characterization	1
1.2	TRH Neuropeptides	2
1.3	FLP Neuropeptides	2
1.4	Neuropeptide Cellular Interaction with Receptors:	3
1.4.1	Endocytosis and Exocytosis Relationship	3
1.4.2	Glutamate Receptors	3
1.5	Modified Neuropeptides	4
2	Methodology	6
2.1	Peptide Preparation	6
2.2	Dielectric Spectroscopy	6
2.2.1	Introduction	6
2.2.2	Experimental Methods	7
2.3	Circular Dichroism	8
2.3.0.1	Introduction	8
2.3.1	Experimental Methods	8
3	Results	10
3.1	Dielectric Relaxation Spectroscopy	10
3.2	Circular Dichroism	13
4	Conclusion	14
	References	15

List of Tables

1	Amino Acid sequence of common peptide residues and corresponding identification information, where MW is molecular weight, μ_E and μ_n are the experimental and theoretical dipole moments, τ is the relaxation time, f is frequency, and ΔH is the activation energy [1]	2
2	Amino Acid sequence of neuropeptides and corresponding identification information	4

List of Figures

1	VMD Computational Models of Modified Scramble, TRH, and FLP families	4
2	Novocontrol Broadband Dielectric Spectrometer	7

3	Graph displaying the alpha, beta, and gamma dispersion processes in Dielectric Spectroscopy. The boxed in frequency range is the range used for this spectrometer model.	8
4	J-1500 series CD spectrometer light path from source to sample. The light source is represented by Ls1 and Ls2, each mirror is represented by M, and the shutter is shown at SH. The light path passes through polarizers denoted by L, F, and CDM	9
5	CD spectra in millidegrees of a model peptide from the J-1500	9
6	Imaginary part of the dielectric permittivity ϵ Permittivity was plotted as a function of frequency for FLP-3-2, FLP-3-9, TRH-1A, and TRH-1B at concentrations of 0.5 μ M and 1 μ M. Due to our low concentrations it is difficult to determine where the alpha and beta processes are located, however differences between the peptides' and concentrations' spectra can be observed.	10
7	Real part of the dielectric permittivity ϵ Permittivity was plotted as a function of frequency for FLP-3-2, FLP-3-9, TRH-1A, and TRH-1B at concentrations of 0.5 μ M and 1 μ M.	11
8	Imaginary part of the conductivity σ Conductivity was plotted as a function of frequency for FLP-3-2, FLP-3-9, TRH-1A, and TRH-1B at concentrations of 0.5 μ M and 1 μ M.	11
9	Real part of the conductivity σ Conductivity was plotted as a function of frequency for FLP-3-2, FLP-3-9, TRH-1A, and TRH-1B at concentrations of 0.5 μ M and 1 μ M.	12
10	Imaginary part of the modulus M was plotted as a function of the real part of the modulus M for FLP-3-2, FLP-3-9, TRH-1A, and TRH-1B at concentrations of 0.5 μ M and 1 μ M.	12
11	CD spectra of the FLP, and TRH families compared to the Scramble	13

1 Introduction

Neuropeptides are a diverse group of polypeptides that can be characterized in different ways. Their properties can depend on the molecular conformation of amino acids and intermolecular forces. FLP and TRH structure function relationship can be inferred based on structure and function of related neuropeptides that are unmodified. There is a strong correlation to the peptide characterization and a cellular entrance pathway. In the following characterizations, we investigate the molecular structure and conformation of neuropeptides to further understand the relationship to the cell entering mechanism.

1.1 Peptide Characterization

The characterization of neuropeptides is heavily dependent on purity, the sequence of amino acid residues, and three dimensional conformation. The three dimensional conformation of the peptide has the greatest effect on function. The conditions that determine a peptides conformation are the pH, temperature, and electrostatic interactions with other molecules. Conformations can take on three forms; the alpha-helix structure, the beta-sheet structure, and linear or random coil structure.

The alpha-helix relies on molecular components to form the structure in aqueous solutions. The alpha-helix secondary structure consists of nitrogen and hydrogen bonds that bind to the carbon and oxygen backbone. The amino acid structure and amount are the first steps to forming the alpha helix [2]. The alpha-helix can also be artificially inserted into a peptide by alanine substitutions since alanine reduces entropy in the peptide side chains and form the curved structure [2].

Beta-sheets are polypeptide β -strands connected by hydrogen bonds. These hydrogen bonds occur at the edges of the sheet structure, and are fundamental for intermolecular forces [3]. These intermolecular forces cause the folds in peptide structure through hydrogen bonding in parallel and anti-parallel forms, and therefore have influence over possible peptide function. Beta-sheets are also responsible for the protein to protein interaction, making these structures a target for signaling processes [3]. Similarly to alpha-helices, beta-sheets can also be artificially created in peptides by replicating amino acid structure that would mimic the same hydrogen bonds formed in related peptides. In addition to beta-sheets, there are also beta-turn structures. These structures connect two other elements of secondary structure based off of the bonds in the first and fourth residue [4]. The beta-turns also commonly involve glycine and proline residues. It is possible that the beta-turns can join two anti-parallel strands and form a beta hairpin structure with stronger intermolecular forces [4]. The properties of the peptide can drastically change if beta-hairpins are formed. This is due to the hairpins having more molecular stability.

Linear structures or Random coils are regions of the protein where secondary structures do not form. Therefore the structure does not have the same hydrogen bonding as seen in alpha-helices or beta-sheets [4]. Random coils are found in the terminal arms of the N-terminus, as well as unstructured loop regions in between other secondary structures [4]. Random coils are found to be as small as four residues long and can be common in smaller peptides.

In addition to secondary structure, there are molecular properties of the residues that can affect conformation and function. The list of common residues and their properties found in neuropeptides in 1. The polarity and angles between atoms are correlated and affect the overall folding structure of the peptide. This was demonstrated in hydrophobic residues being the controlling factor of the folding structure in water soluble proteins [5]. There are

also complications regarding the nonuniform polarity of the residues. For example, there can be cases where a residue facing into the protein will have a polar region and nonpolar side chains facing the solvent and therefore the polarity varies widely across the residue [5].

Table 1: Amino Acid sequence of common peptide residues and corresponding identification information, where MW is molecular weight, μ_E and μ_n are the experimental and theoretical dipole moments, τ is the relaxation time, f is frequency, and ΔH is the activation energy [1]

Amino Acid	Polarity	MW	μ_ϵ (D)	μ_η (D)	τ (ps)	f (GHz)	ΔH
Glycine	-	75	15.5	15.0	49	3.23	18.6
α - Alanine	-	89	17.7	16.8	92	1.72	15.9
Valine	-	117	17.4	16.7	107	1.48	16.2
Proline	-	115	18.4	17.6	112	1.42	17.2
Lysine	+	146	25.0	23.6			
Histidine	+	155	27.3	35.6	-	-	-
Arginine	+	174	33.8	30.4			
di-Glycine	NP	130	29.1	-	-	-	-
Glycyl-Alanine	NP	146	30.8	-	170	0.94	16.8
tri-Glycine	NP	189	36.8	-	258	0.62	18.7

(REF VAL 232)

1.2 TRH Neuropeptides

Thyrotropin releasing hormone (TRH) is a family of neuropeptides with a general sequence of pGlp-His-Pro-NH₂. TRH main interaction with the cell membrane is through G-protein coupled receptors, with some receptors showing stronger constitutive activity than others depending on the organism [6]. This variation in TRH activity suggests that each receptor on the plasma membrane completes a different function in response to TRH. Specifically in *C. elegans*, TRH peptides bind to the receptor TRHR-1 to promote growth and motion [6]. There is a multistep process for TRHs to produce a function in the brain’s pituitary gland. TRH interacts with exonucleases that hydrolyze peptide bonds. Specifically, the bond between the N-terminal pyroglutamate acid and the histidine residue is hydrolyzed [7]. This process results in a dipeptide amine (His - Pro) which is spontaneously cyclized into a His-Pro diketopiperazine (DKP). Unlike the original TRH neuropeptide, DKP does not have the thyroid stimulation activity, and can inhibit prolactin used from the pituitary gland [7]. Altering the structure of TRHs could affect the prolactin inhibition or partial inhibition.

1.3 FLP Neuropeptides

A group of neuropeptides commonly found in *C. elegans* called FMRFamide-related peptides (FaRPs) are a baseline for deriving the FLP family of genes. The group of FaRP genes found in *C. elegans* all share a similar amino acid sequence of Arg-Phe-Gly starting with a custom N- terminus and ending with a C-terminus [8]. FaRP genes with this specific structure are known as FLP genes. Modification on different amino acids in the peptide sequence can alter the peptide’s function, and therefore investigation of each individual FLP sequence and alteration must be performed.

Based on the modification of the FLP neuropeptide it is possible that there are slight changes in binding affinities

to cell receptors. For example, certain N-terminal extensions can form secondary protein structures that decrease affinity and therefore can decrease function within the cell [8].

1.4 Neuropeptide Cellular Interaction with Receptors:

In order for neuropeptides to have an effect in signaling behavior through neurons, they must first have a way to pass through the neuronal or synaptic membrane. There are multiple signal pathways and receptors that neuropeptides bind to based on their configuration, charges, and concentrations. If the peptide successfully binds to the receptor, then the peptide can cross the membrane where it can then signal other cascades that result in behavioral function. If the conditions for internalization are not met because of the peptide conformation the peptide will not be able to enter or leave the cell in the current form.

1.4.1 Endocytosis and Exocytosis Relationship

Endocytosis and exocytosis are both mechanisms of materials crossing the cell membrane through molecular signals into a transport vesicle. Specifically, receptor mediated endocytosis of neuropeptides has the mechanism for the entering and leaving being dependant on voltage gated ion concentrations and peptide receptors on either side of the membrane. For TRH, the exocytosis is strongly dependant on voltage clamp pulses with Ca^{2+} and temperature, while endocytosis is also strongly dependant on Ca^{2+} generated [9]. In addition to the endocytosed vesicles that TRH travels in there are protein receptors that assist internalization of TRH. lactotrope and thyrotrope receptors rapidly internalize TRH into endosomes at high temperatures [10]. This endocytosis also revealed that TRH Ca^{2+} dependency is based on the TRH receptors [10].

Different peptides can have different modes of endocytosis or exocytosis. For FLP, receptor mediated endocytosis is also shown through a different set of receptors, however these receptors are still a topic of investigation.

1.4.2 Glutamate Receptors

Neuropeptides can be endocytosed through the synaptic membrane glutamate receptors. Glutamate receptors are classified as ligand gated ion channels and G-protein coupled receptors, where both are responsible for neuropeptide functionality. Neuropeptides interact with membrane bound G-protein coupled receptors (GPCRs). GPCRs work through signal transduction coupling to a variety of other proteins leading to the activation of effector molecules [11]. The signal cascade from a GPCR functions with additional membrane ion channels. The major receptor responsible for endocytosis in the synapse is the N-methyl-D-aspartic acid receptor (NMDA) that coincides with lipid rafts in the transport of neuropeptides [12]. Small segments of peptide DNA trigger a receptor reaction to endocytose the peptide. The NMDA receptor allows for endocytosis which then starts a signal cascade to possibly allow other peptides to be endocytosed simultaneously through other receptors [12]. In addition, integrins that regulate cellular proliferation and apoptosis are associated with NMDA lipid rafts. Some neuropeptides like AB bind to integrins directly in order to regulate the neurotoxic effects of AB. The NMDA, lipid rafts, and integrins are plausible intake methods for AB and other neuropeptides, or these methods would trigger an additional signal cascades following activation of these previous receptors.

Another glutamate receptor responsible for neuropeptide uptake is -amino-3-hydroxyl-5-methyl-4-isoxazole-propionate receptor (AMPA). The AMPA and NMDA receptors can be co-expressed by the same glutamatergic synapse with similar relation to lipid rafts (X). One difference is that the AMPA receptor can be recycled relatively fast from the synapse surface. The fast recycling is indicative of AMPA being a more efficient carrier of neuropeptides. As

an example, AB was tested with AMPA receptors, and showed that AMPA receptor trafficking is regulated by small segments of AB peptide (x.). AMPA is a highly likely carrier for AB and therefore can assume with similar structure, other families of neuropeptides can use this uptake pathway.

1.5 Modified Neuropeptides

The TRH and FLP neuropeptide sequence was modified to include point mutations and insertion mutations to determine structural differences between the sequences of the same family. Specifically, the mutations occur in the TRH peptides where the Arginine and Glycine in TRH-1A were substituted with asparagine and alanine in TRH-1B. In the FLP family, a point mutation was made with the leucine in FLP-3-2 changing to a phenylalanine. There is also an additional tail of five residues added to FLP-3-9 that starts with aspartic acid and continues with asparagine, glutamic acid, proline, and asparagine. These modifications are highlighted in Table 2. The models of each neuropeptide can be found in Figure 1.5. where the residues are labeled by location on the peptide. The secondary structure is also indicated by the color change where white is a random coil, blue is a beta structure, and purple is the alpha-helix structure. Additionally all modified sequences have identical N terminus before residue 1 and C terminus after the final residue listed.

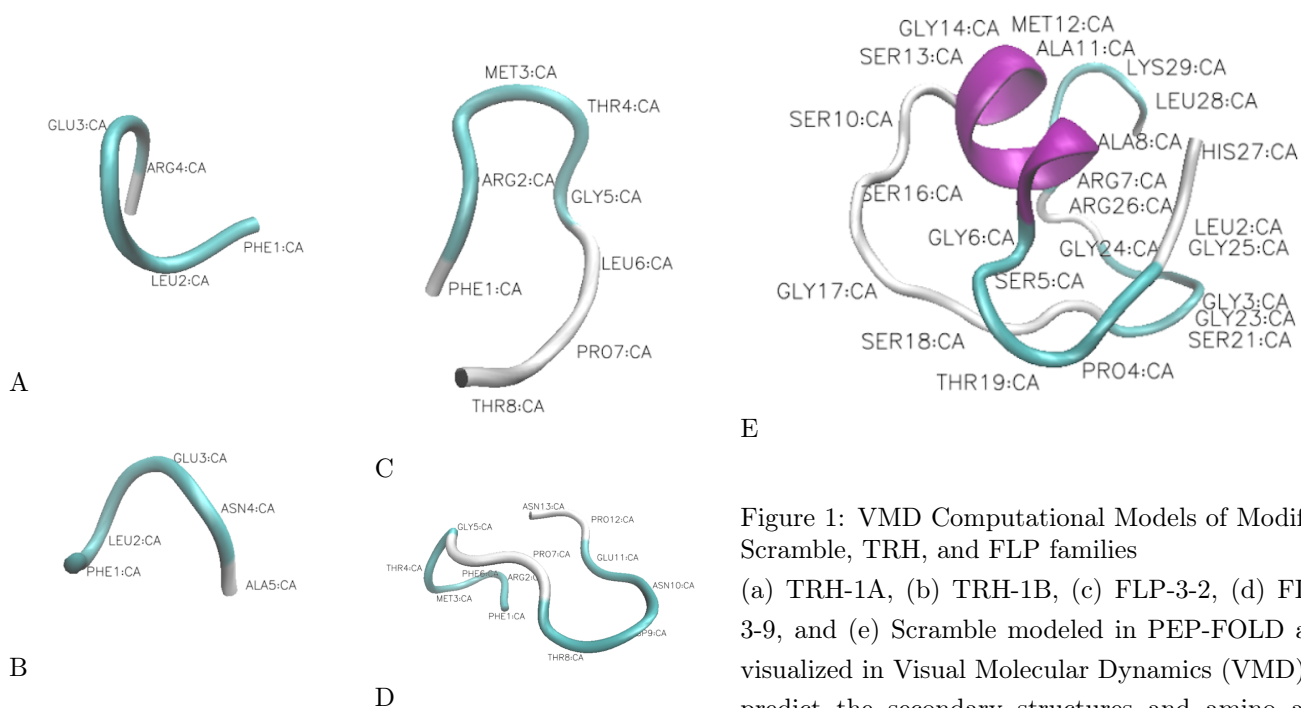


Figure 1: VMD Computational Models of Modified Scramble, TRH, and FLP families (a) TRH-1A, (b) TRH-1B, (c) FLP-3-2, (d) FLP-3-9, and (e) Scramble modeled in PEP-FOLD and visualized in Visual Molecular Dynamics (VMD) to predict the secondary structures and amino acid interactions[13][?].

Table 2: Amino Acid sequence of neuropeptides and corresponding identification information

Neuropeptide	Sequence	Molecular Weight (g/mol)	PI	Average ϕ
SCRAMBLE	NH ₂ -QLGPSGRAHSAMSGTSGSTRSRGGGRHLKSN-COOH	3213.4234	12.48	7
TRH-1A	NH ₂ -FLE RG -COOH	738.7534	6.00	0
TRH-1B	NH ₂ -FLE NA -COOH	710.6934	4.00	-1
FLP-3-2	NH ₂ -FRMTG L P T -COOH	1040.1734	9.75	1
FLP-3-9	NH ₂ -FRMTG F P T D N E P N -COOH	1643.7234	4.37	-1

2 Methodology

In this section, we overview the two methods used to collect data on our peptide samples: Dielectric Relaxation Spectroscopy and Circular Dichroism. We also provide an overview of the methods used in the IGOR Pro 6 software to read the spectra and plot our figures.

2.1 Peptide Preparation

Peptide samples were obtained from Professor Srinivasan's lab at WPI and included: crude FLP-3-2, FLP-3-9, TRH-1A, and TRH-1B all at $1\mu\text{M}$; pure FLP-3-2, FLP-3-9, TRH-1A, and TRH-1B at both $1\mu\text{M}$ and $2\mu\text{M}$; and the background, water for molecular biology from Millipore. The samples were all stored at -20°C inside 2mL Biomatik microcentrifuge tubes in the Millipore water medium. Samples were extracted using a $200\mu\text{L}$ pipette tip and if needed were diluted in a separate microcentrifuge tube using the Millipore water.

2.2 Dielectric Spectroscopy

2.2.1 Introduction

Dielectric spectroscopy is a method of measurement in which the principles of dielectric polarization is used to classify the properties of sample materials by treating them as a dielectric. An electric field induced on a sample will result in the bound charges within to orient themselves parallel to the electric field, and the positive free charges to attract in the direction of the field (and the negative charges, vice versa). A time-dependent electric field is used to create a spectrum across a large frequency range, where [1]

$$\mathbf{P}(\mathbf{t}) = \varepsilon_0\chi\mathbf{E}(\mathbf{t}) \quad (1)$$

where

$$\chi = \varepsilon_l - 1 \quad (2)$$

and

$$E^*(t) = E_0e^{i\omega t} \quad (3)$$

After introducing the displacement field the equation will fall into the form

$$D^*(\omega) = \varepsilon_0\varepsilon^*(\omega)E^*(\omega) \quad (4)$$

and by using Euler's relations, we find

$$\varepsilon^* = \varepsilon_{real} - i\varepsilon_{img} \quad (5)$$

which gives the representation of the complex dielectric permittivity. Dielectric spectroscopy directly measures the impedance of the sample, which is inversely proportional to the complex permittivity. The permittivity can then be used to find a different quantities, including the complex conductivity, complex modulus, and dielectric relaxation time. The conductivity and modulus are given as follows: [1][14][15]

$$M^* = \frac{1}{\varepsilon^*} \quad (6)$$

$$\sigma^* = i\omega\varepsilon_0\varepsilon^* \quad (7)$$

and the relaxation time is denoted by τ .

Aside from the dielectric permittivity spectra, we chose to present the conductivity and modulus spectra as our secondary formalisms. Modulus graphs are especially useful for samples where free charges are more prevalent, as at low frequencies the effects of conductivity can obscure the processes in permittivity spectra. Taking the inverse of permittivity reduces the effects of conductivity on the curve and allows for easier fitting (paper). The modulus representation also holds higher frequencies at greater weight as the peaks will be shifted to a slightly higher frequency [14].

2.2.2 Experimental Methods

We used the Novocontrol Broadband Dielectric Spectrometer 2 to test the dielectric properties of our samples on the frequency range 200mHz to 40MHz based on Figure 3. We used a cylindrical liquid sample cell to load our peptide solutions. For each experiment, we measured 0.6mL of sample at both 1 μ M and 0.5 μ M concentrations and took 4 spectra of each sample to check for consistency. The WINDETA software was used to operate the spectrometer, and following experiments the data was analyzed using IGOR Pro. The same concentrations of both FLP peptides were graphed together, as well as the same concentrations of both TRH peptides, and all were plotted against the deionized water background.



Figure 2: Novocontrol Broadband Dielectric Spectrometer

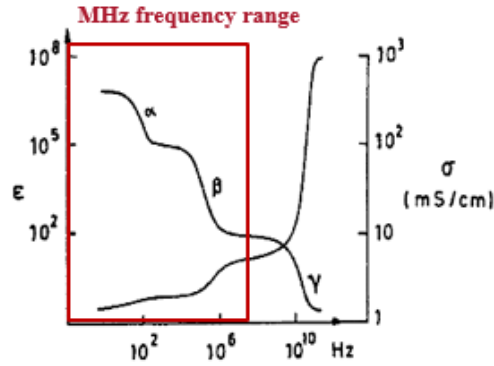


Figure 3: Graph displaying the alpha, beta, and gamma dispersion processes in Dielectric Spectroscopy. The boxed in frequency range is the range used for this spectrometer model.

2.3 Circular Dichroism

2.3.0.1 Introduction

Circular dichroism is a spectroscopy method which utilizes the asymmetry of atoms and molecules to produce a unique spectrum based on structure. Specifically, the structure of a carbon atom is asymmetrical, or "chiral". Similarly, the amino acids that build into protein molecules contain asymmetries in structure. Therefore, proteins, being constructed out of amino acids and carbon, will have different asymmetries based upon composition which can be measured to provide a structural approximation. Circular dichroism itself is a method which exposes a sample to both left- and right- circularly polarized light, and returns a measure of the difference in absorption between the two, as shown by: [16]

$$\Delta A = A_L - A_R \quad (8)$$

2.3.1 Experimental Methods

To further understand the peptide structures, we used circular dichroism to determine the alpha, beta, and random coil structures of each neuropeptide. The CD instrument we used was the JASCO, J-1500 series spectrometer 4 with LAB4US 3-Q-10 quartz cuvettes for measuring in the UV spectra. To begin reading data, the J-1500 requires coolant, 10psi nitrogen gas, and the light shutter open. For the sample loading, we measured 2mL of neuropeptide at 2 μ M concentration in DI water in the 3-Q-10 cuvette and loaded the cuvette into the J-1500 chamber.

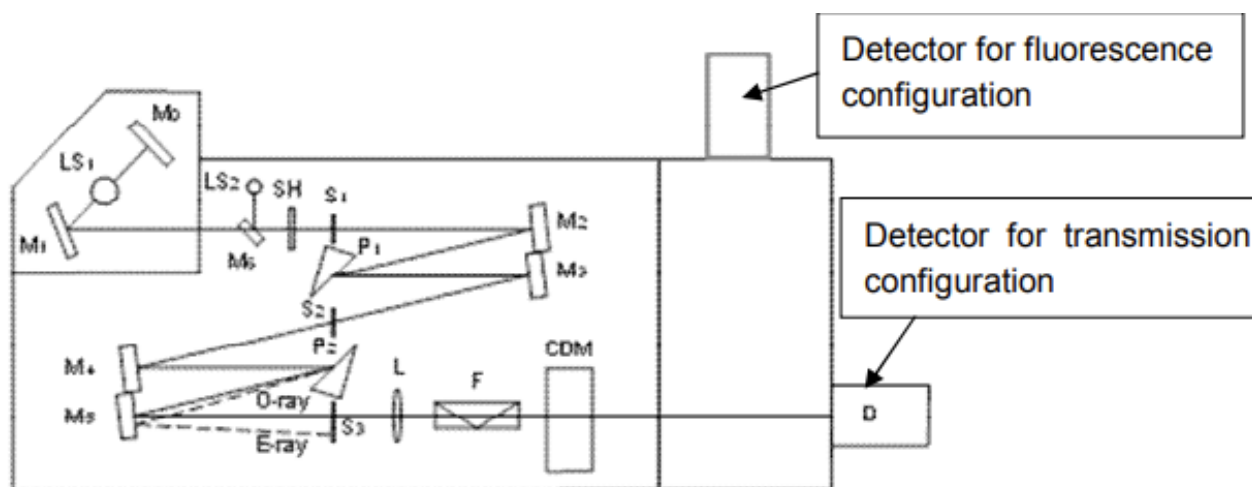


Figure 4: J-1500 series CD spectrometer light path from source to sample. The light source is represented by Ls1 and Ls2, each mirror is represented by M, and the shutter is shown at SH. The light path passes through polarizers denoted by L, F, and CDM

In SpectraManager™ software, the settings were adjusted so our wavelength range would be taken from 190nm to 240nm in 0.1nm increments. Additionally, we set the CD to average 30 cycles of data on each neuropeptide to minimize interference outliers and average the data. Each neuropeptide was also plotted against the background Millipore Nuclease Free water at the beginning of each test. The resulting data was given in millidegrees vs. wavelength where we would measure the positive and negative bands of each peptide curve. We based the characterization of these bands based on Figure 5.

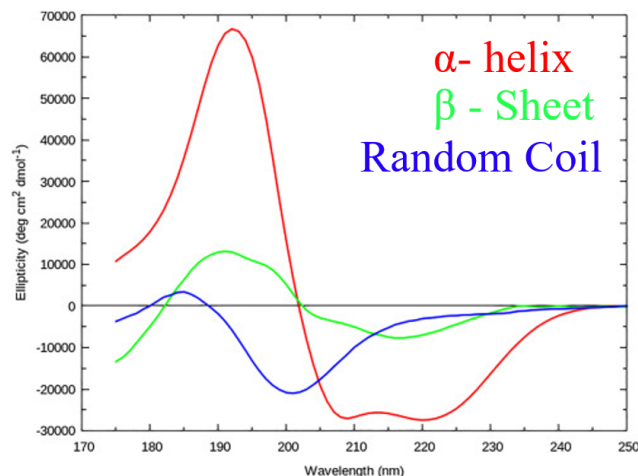


Figure 5: CD spectra in millidegrees of a model peptide from the J-1500

Depending on the secondary structure, there are distinguishable positive and negative bands. We determined each of the modified peptides had similar positive and negative bands as represented by this model. To evaluate the positive and negative peaks, we plotted the SpectraManager™ results into IGBOR exactly as shown for DRS.

3 Results

3.1 Dielectric Relaxation Spectroscopy

Figures 6 and 7 show both parts of the complex permittivity as a function of frequency. Figures 8 and 9 show both parts of the complex conductivity as a function of frequency. Figure 10 shows the imaginary modulus plotted against the real modulus, known as a Cole-Cole plot. With this small of a peptide and low of a concentration, we do not expect to see the dielectric processes themselves, however structural differences can be inferred between peptides based off the difference in spectra.

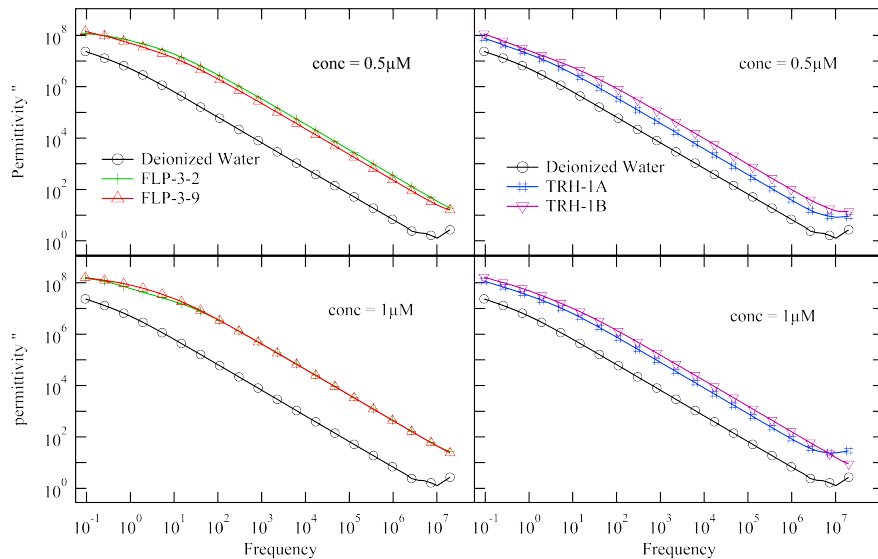


Figure 6: Imaginary part of the dielectric permittivity ϵ'' Permittivity was plotted as a function of frequency for FLP-3-2, FLP-3-9, TRH-1A, and TRH-1B at concentrations of $0.5\mu\text{M}$ and $1\mu\text{M}$. Due to our low concentrations it is difficult to determine where the alpha and beta processes are located, however differences between the peptides' and concentrations' spectra can be observed.

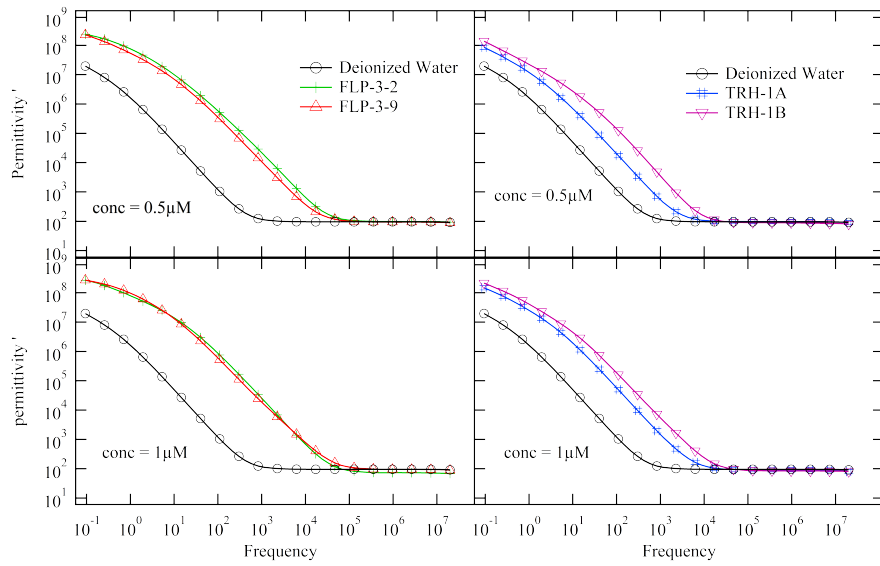


Figure 7: Real part of the dielectric permittivity ϵ' Permittivity was plotted as a function of frequency for FLP-3-2, FLP-3-9, TRH-1A, and TRH-1B at concentrations of $0.5\mu\text{M}$ and $1\mu\text{M}$.

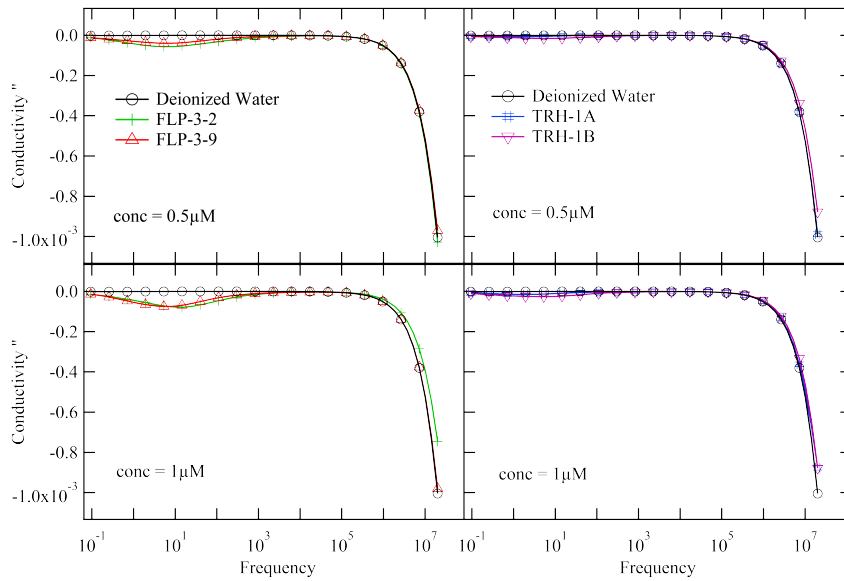


Figure 8: Imaginary part of the conductivity σ'' Conductivity was plotted as a function of frequency for FLP-3-2, FLP-3-9, TRH-1A, and TRH-1B at concentrations of $0.5\mu\text{M}$ and $1\mu\text{M}$.

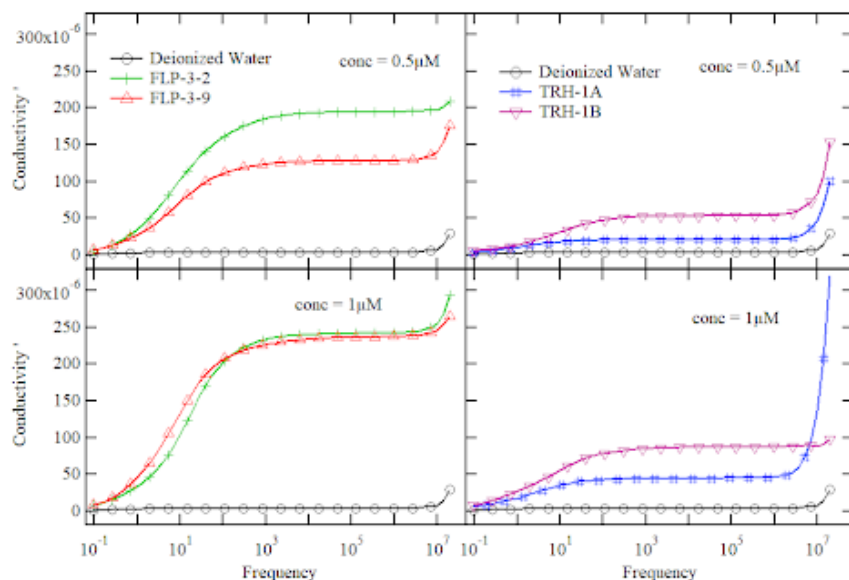


Figure 9: Real part of the conductivity σ' was plotted as a function of frequency for FLP-3-2, FLP-3-9, TRH-1A, and TRH-1B at concentrations of $0.5\mu\text{M}$ and $1\mu\text{M}$.

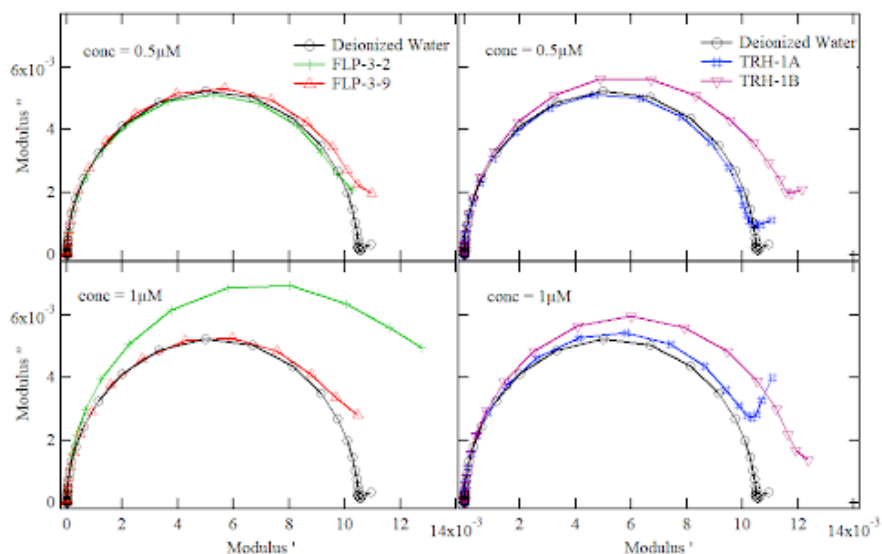


Figure 10: Imaginary part of the modulus M'' was plotted as a function of the real part of the modulus M' for FLP-3-2, FLP-3-9, TRH-1A, and TRH-1B at concentrations of $0.5\mu\text{M}$ and $1\mu\text{M}$.

We found differences in the complex dielectric permittivity, especially pronounced in the real part, for both samples at both concentrations. Differences tended to be more pronounced in the $0.5\mu\text{M}$ concentration than in the $1\mu\text{M}$. For FLP-3-2, differences were more pronounced in the modulus plot; the $1\mu\text{M}$ concentration showed departure from the rest of the samples. Amino acids' polar nature on their side chains allows us to study their dielectric properties in aqueous solution. While in our frequency range amino acid chains have similar dielectric processes to water, we can see differences in behavior here in the magnitude of the dielectric permittivity. It is possible that the differences between the $1\mu\text{M}$ and $0.5\mu\text{M}$ experiments are due to interactions between the solute molecules becoming more constant at higher concentrations.

3.2 Circular Dichroism

The CD spectra of the FLP, TRH, and scramble peptides shown in 11 can be compared to the VMD images in Figure 1.5. The high and low peaks of the scramble are reminiscent of some combination of all three structures types (alpha helix, beta structures, and random coil), which conforms with our earlier model. TRH-1A closely follows the curve of a random coil, and TRH-1B looks most similar to a combination of random coil and beta sheet. While the TRH-1B data looks just as we would expect based on the VMD simulation, the spectra of TRH-1A does not show the expected beta sheet structure. Finally, both FLP peptides have spectra reminiscent of a primarily beta sheet structure, as the negative peaks amplitude is too low to suggest an alpha helix.

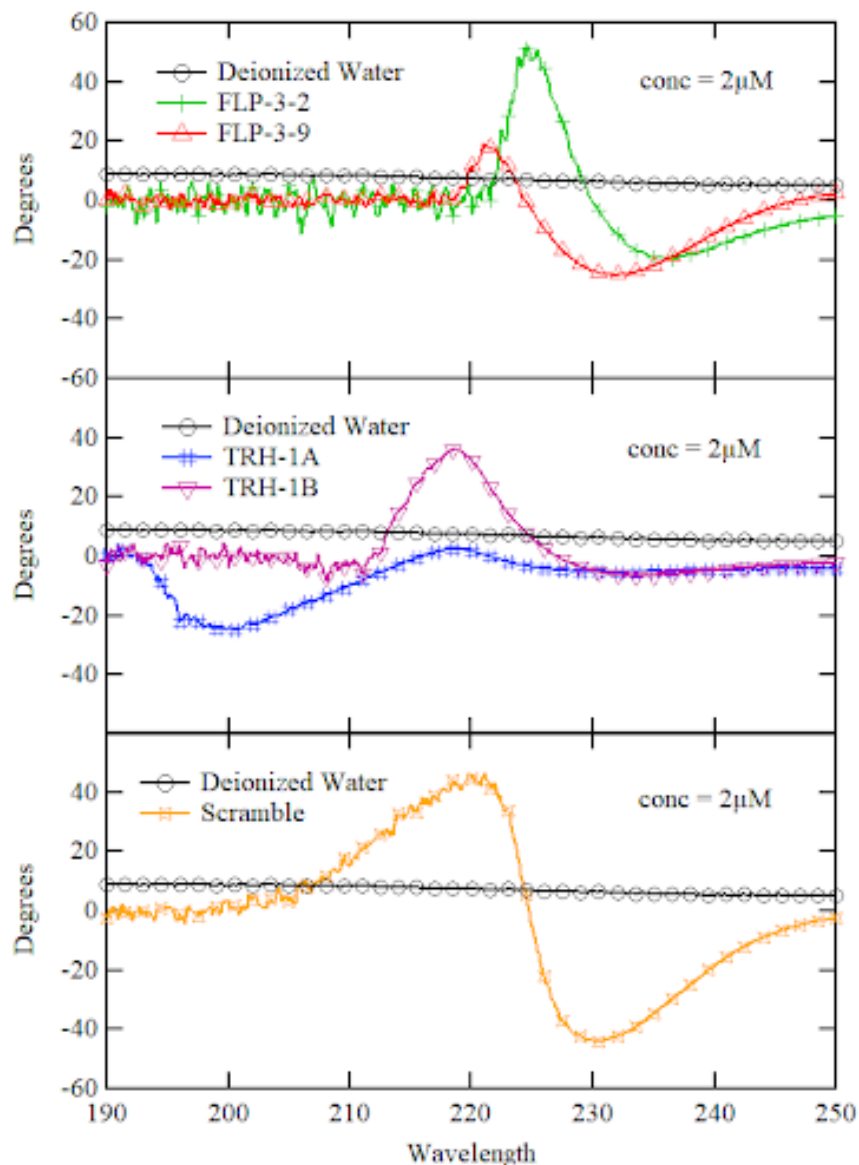


Figure 11: CD spectra of the FLP, and TRH families compared to the Scramble

4 Conclusion

We investigated the structure-function relationship of the FLP and TRH peptide families using Dielectric Relaxation Spectroscopy and Circular Dichroism. We measured the Dielectric Permittivity and CD spectra of the peptides at different concentrations. We found agreement between the CD spectra and predicted VMD computational structure. The DRS data shows departure in modulus and conductivity with the FLP family between the two concentrations. For the TRH family, the peptides display different conductivity and modulus from one another, while showing similar behavior at different concentrations. Our results support recent research showing that a change in the amino acid sequence exhibits different electrostatic forces, which will alter the cell entering mechanism. Future work on this topic includes taking data at a variety of peptide concentrations to better understand the trends observed here in the FLP peptide family. In addition, in order to understand the cell entering mechanism, experiments related to neuropeptides in cells should be performed.

References

- [1] Y. Feldman and V. Raicu, *Dielectric Relaxation in Biological Systems: Physical Principles, Methods, and Applications*. OUP Oxford, 2015.
- [2] Y. G. H. Z. N. R. K. J Yang, E J Spek, “The role of context on a-helix stabilization:host-guest analysis in a mixed background peptide model,” *Protein Science*, 1997.
- [3] N. JS., “Exploring beta-sheet structure and interactions with chemical model systems,” *Acc Chem Res.*, 2008.
- [4] S. Everse, “Secondary structure (2) – beta turns and random coils,” 2014.
- [5] J. Manor, E. S. Feldblum, M. T. Zanni, and I. T. Arkin, “Environment polarity in proteins mapped noninvasively by ftir spectroscopy,” Mar 2012.
- [6] P. M. Hinkle, A. U. Gehret, and B. W. Jones, “Desensitization, trafficking, and resensitization of the pituitary thyrotropin-releasing hormone receptor,” Jan 2012.
- [7] J. F. MvKelvy and S. Blumberg, “Inactivation and metabolism of neuropeptides,” *Annual Review of Neuroscience*, vol. 9, pp. 415–434, 1986.
- [8] C. Li and K. Kim, “Family of flp peptides in caenorhabditis elegans and related nematodes,” Oct 2014.
- [9] A. Fomina and E. Levitan, “Three phases of trh-induced facilitation of exocytosis by single lactotrophs,” *The Journal of Neuroscience*, vol. 15, no. 7, p. 4982–4991, 1995.
- [10] R. YU, R. ASHWORTH, and P. M. HINKLE, “Receptors for thyrotropin-releasing hormone on rat lactotropes and thyrotropes,” *Thyroid*, vol. 8, p. 887–894, Nov 1998.
- [11] Y. Zhang, Z. Wang, G. S. Parks, and O. Civelli, “Novel neuropeptides as ligands of orphan g protein-coupled receptors,” Feb 2011.
- [12] A. Y. Lai and J. McLaurin, “Mechanisms of amyloid-beta peptide uptake by neurons: The role of lipid rafts and lipid raft-associated proteins,” Dec 2010.
- [13] S. Humphrey W, Dalke A, “Visual molecular dynamics,” *Journal of Molecular Graphics Modelling*, vol. 14, pp. 33–38, 1996.
- [14] *Broadband Dielectric Spectroscopy*. Springer, 2012.
- [15] G. M. TSANGARIS, G. C. PSARRAS, and G. M. TSANGARIS, “Electric modulus and interfacial polarization in composite polymeric systems,” *Journal of Materials Science*, vol. 33, no. 8, p. 2027–2037, 1998.
- [16] B. A. Wallace and R. W. Janes, *Modern Techniques for Circular Dichroism and Synchrotron Radiation Circular Dichroism Spectroscopy*. IOS Press, 2009.